

# Exploring the Complex Welding Engineering Design Space using Computational Weld Mechanics

Mahyar Asadi<sup>1</sup>, Mike Shubert<sup>2</sup>, Majid Tanbakuei Kashani<sup>1</sup>, and Mathew Smith<sup>1</sup>

1. Applus Canada – Vancouver Office, 19165 94th Avenue, Surrey, BC, Canada, V4N 3S4  
[Mahyar.Asadi@applusrtd.com](mailto:Mahyar.Asadi@applusrtd.com)
2. SIMULIA South – Dassault Systemes Dallas Mountain Southwest Area, 220 E. Las Colinas Blvd., Suite 1150, Irving, TX, US, 75039

**Abstract:** *The use of computational models is well established in many areas of engineering; however the welding is among few fields where design and designer-driven control and optimization remain generally traditional. For example, weld distortion is a frequent problem in various welding applications including additive manufacturing and many techniques have been developed over time to mitigate the distortion. Welding sequence and intermittent welding design, which determine the best welding pattern in multi-pass welds, are familiar techniques to control the distortion when dealing with multi-pass welded structures. Finding the best solution for such a design is limited by available resources since a designer needs to pick one out of many patterns i.e. hundreds to thousands patterns, usually based on experience. Optimization of this problem is not feasible through shop trials, so we use computer modeling that supports implementation of several patterns for minimal distortion. Practical solutions will be found if a service provider becomes skillful in handling significantly large number of modeling analyses in a short time frame. This approach helped clients to define an optimal design envelope with a clear understanding of the correlation between large numbers of design parameters – the only feasible approach to exploring the complex welding engineering design space.*

**Keywords:** *Computational Weld Mechanics, Welding Distortion, Welding Modeling and Simulation, Weld Sequence Design, Mitigation of Distortion.*

## 1. Introduction

Welding comprises a significant portion of manufacturing, fabrication and erection of structures around us where the art of welding is being continuously advanced by welding science and engineering. Welding is the main focus of metallic fabrication because of the high flexibility and production speed. However, weld is frequently presented as the critical part of structures where the local thermal, microstructural, and mechanical change in the weld region lead to a sub-optimal properties and service condition that are usually undesirable. A large variety of advanced materials have been developed and structures are designed using these materials to tolerate severe service conditions. Still failures are observed in such structures and are frequently reported to occur in the weld region, sometimes after a relatively low in-service life.

The reason is because we are taking the weld for granted in many disciplines of engineering. Generally, the weld engineers rely on previous experience and the best practice of moment – a non-deterministic trial and error approach. That is why car's integrity is linked to weld resistance to rupture in the crash, and the degree of reliability is defined by the welds. New materials such as Aluminum, Magnesium, and High Strength Steels are now available to improve power-to-weight ratio in cars, however, their welding concerns prevent them yet from seeing them in our streets. Broken welds are the biggest cause of train derailments as of claim by the Federal Rails Transportation. Historically, weld issues have repeatedly delayed manufacturing of new rail cars, as well as fatigue in existing rail cars, are frequently reported on welds. Welding forms a significant portion of shipbuilding where the weld distortion is now the major challenge of shipyards around the world. Every year, hundreds of wonky welds keep marine fleets stuck in port. Although welding is the fastest method of fabrication, the use of welding in the aircraft industry has been restricted, in general, due to the lack of fully reliable welding. Fusion line fracture is a known problem of 3D printed products that are ranked highly prone to cracking in long-term service condition under fatigue and creep. The pipeline, energy, oil and gas industries recognize weld as the most fragile bottleneck of manufacturing and fabrication. Many controversy around pipelines root in unreliability and failure in weld not the pipeline. Our energy infrastructure are made of very good failure resistance materials but they fail in weld region when welded. If we believe the green projects are essential for our environment on one hand and the safety of our workforce and safeguarding public are our due diligence on another hand, Welding is the key manufacturing segment to reduce hazards to our environment and enhanced safety to the workforce and safeguarding the public. The bottleneck that is complex engineering in nature because the science of welding is complex and our engineers are not equipped with proper tools that enables them for designer-driven optimization of welded structures and related welding procedures. Using the high performance computing platform for simulation and weld modeling, combined with practical experience, welding engineers will be capable of applying their creativity, expertise and skill to be optimal, more productive, and innovative when developing solutions to welding problems.

Weld distortion is the most frequent problem in welding applications and many techniques have been developed over time to mitigate distortion or in some case achieve zero distortion (Asadi & Goldak, 2013) and (Yang & Jung, 2007). Simple techniques like tack welding and fixturing can now be optimized using welding models that reliably predict distortion (Wang & Rong, 2008). Furthermore, simulation and modeling enables the designer to optimize complex methods like pre-offset (Asadi & Goldak, 2011), transient side heating (Conrardy, et al., 2006), reverse heating (Mochizuki & Toyoda , 2006), dynamic tensioning (xu & Li, 2006), or more advanced techniques including adaptive clamping (Schenk, Richardson, Kraska, & Ohnimus, 2009) and adaptive process control (Asadi, Goldak, & Weck, 2014).

Welding sequence and intermittent welding design, which determines the best welding pattern in multi-pass welds, are familiar techniques to control the distortion when dealing with multi-pass welded structures. Finding the best solution for such a design is limited by available resources since a designer needs to pick one out of many patterns i.e. hundreds to thousands patterns, usually based on experience. Optimization of this problem is not feasible through shop trials, so the best available alternative is to use computer modeling that automates implementation of several patterns for minimal distortion, residual stress, or other design objectives. When combined with optimization algorithm and technique, it can efficiently select the best pattern out of tens of thousands of pattern or all possible weld sequence configurations. Genetic algorithm (Kadivar, Jafarpur, & Baradaran,, 2000), joint rigidity method (Tsai, Park, & Cheng, 1999), and Surrogate modeling (Voutchkov, Keane, Bhaskar, & Olsen, 2005) and (Asadi & Goldak, 2011) are among successful algorithms for defining the best weld sequence in multiple weld structures.

As mentioned earlier, using a high performance computing platform for simulation and weld modeling that automates multiple setups and evaluations is an essential tools for practical implementation of these techniques. Saving an expert-user's time to prepare several analyses and allocating CPUs to be utilized efficiently make these techniques cost effective and time effective to manage industrial-scale designer-driven optimization and control application of weld modeling and simulation.

## 2. 3D Simulation Model

A full 3D idealized model of a panel structure shown in Figure 1 was created including 7 panels that were fillet-welded on the flat base plate with 84 weld passes and 52 tack welds for initial positioning of panels on the base plate before welding starts. Single-bead weld passes were deposited with average leg size equal to 15 mm. Although a weld bead of this size may be cause difficulties welding physically, its dimensions were chosen for aesthetic reasons. This geometry is idealized and is intended for instructional purposes only. The overall dimension of the base plate is 4000x3000x50 mm, the mid panel 2600x450x50 mm, the largest side panels 1667x432x25 mm, the middle side panels 1460x400x25 mm, and the smallest side panels 1083x342x25 mm. The mesh employed is shown in Figure 1 and has 54,001 nodes and 35,036 elements which assigned to 8-node linear heat transfer brick (DC3D8) for thermal analysis. The main consideration of the model for transient thermal analysis is described further in this paper. The analysis uses temperature-dependent properties. The panel is made of mild carbon steel with 0.15 wt% C, 1.35 wt% Mn, and 0.28 wt% Si, and the temperature-dependent material properties are given in Table 1. Because of the oversized weld bead, a somewhat unrealistic set of torch parameters was used: 400 [amp], voltage 36 [v], travel speed 5.0 [mm/s], efficiency 0.7. There was 2 seconds of initial torch heat up time and 2 seconds hold time between the weld passes.

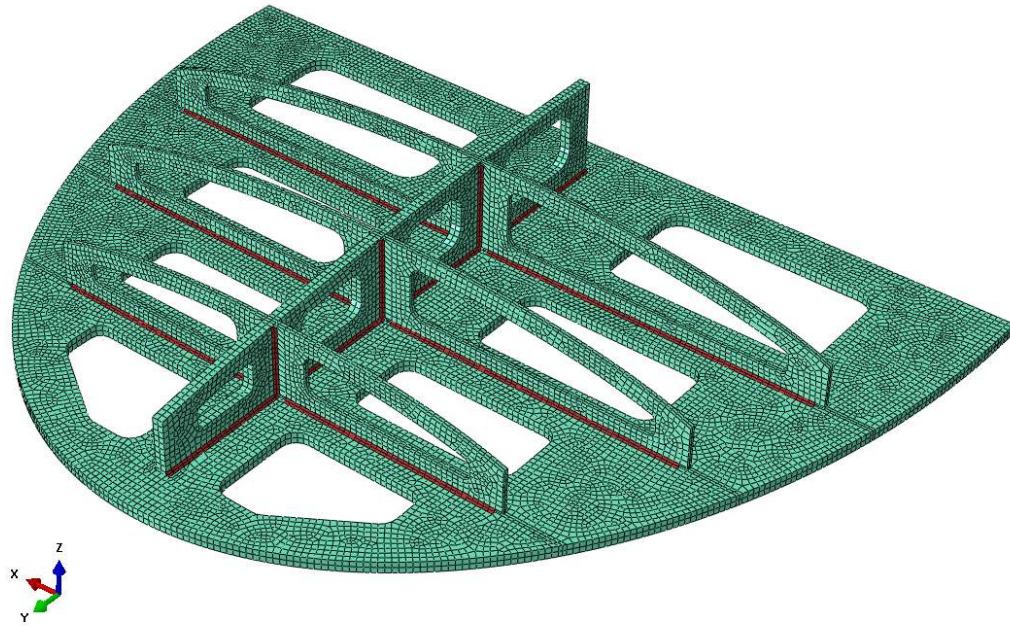


Figure 1: Welding Modeling Panel.

Table 1 Temperature dependent material properties used in the model.

Temperature (C)	Specific Heat (mJ/tonne C) xE+6	Conductivity (mJ/mm C s)	Density (tonne/mm <sup>3</sup> ) xE-9	Yield Stress (MPa)	Thermal Expansion Coefficient (C-1)	Young's Modulus (GPa)	Poisson Ratio
0	400	40	8.06	250	1.30435E-05	210	0.33
100	460	40	8.02	232	1.30435E-05	209	0.33
200	530	40	7.99	209	1.30435E-05	204	0.33
300	600	39	7.95	183	1.30435E-05	194	0.33
400	660	38	7.92	152	0.0000133	181	0.33
500	730	37	7.88	118	0.0000135	164	0.33
600	800	36.5	7.85	79	0.0000137	143	0.33
700	860	36	7.81	37	0.0000139	118	0.33
800	1300	35.5	7.78	19	1.47657E-05	89	0.33
900	1200	35	7.82	12	1.64081E-05	55	0.33
1000	1100	34.5	7.79	8	1.79607E-05	27	0.33
1100	990	34	7.74	5	1.94133E-05	16	0.33
1200	880	33.5	7.66	4	2.07559E-05	11	0.36
1300	780	33	7.57	3	2.19784E-05	5	0.41
1500	600	32	7.3	2	2.4023E-05	1	0.48

### 3. Thermal Analysis

A full 3D model of panel was created using Abaqus Welding Interface 2017 (AWI). The welding torch is simulated through the double ellipsoid heat source model of Goldak (see Figure 2) where the element fluxes are calculated from Eq. 1 to 3 for each ellipsoid. The AWI has implemented this through the user subroutine UMDFlux. Many arguments are passed to this user-subroutine including the element number, element volume, time at the beginning and end of the increment. The AWI uses the times at the beginning and end of the increment and the torch positions at the beginning and end of the increment to compute the integrated flux of the time increment. That total flux value is then divided by the element volume and time increment to return the energy per unit volume per time. Double Ellipsoid model are chosen 15, 15, 15, and 30 mm for a, b, cf, and cr respectively. These numbers are adjusted to best present the cross section of weld modeled.

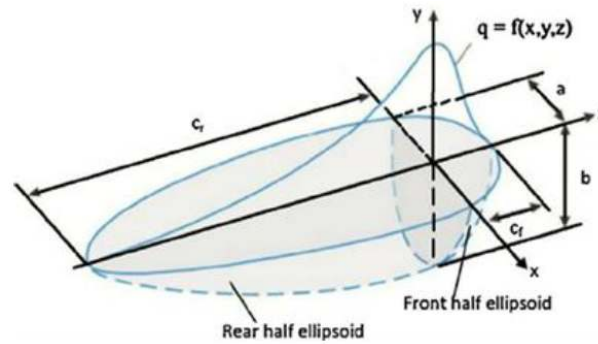


Figure 2: Double Ellipsoid Model of Goldak.

$$q_r(x, y, z) = \frac{6\sqrt{3} f_r Q}{abc_r\pi\sqrt{\pi}} e^{\left(\frac{-3x^2}{a^2}\right)} e^{\left(\frac{-3y^2}{b^2}\right)} e^{\left(\frac{-3z^2}{c_r^2}\right)} \quad \text{Eq. 1}$$

$$q_f(x, y, z) = \frac{6\sqrt{3} f_f Q}{abc_r\pi\sqrt{\pi}} e^{\left(\frac{-3x^2}{a^2}\right)} e^{\left(\frac{-3y^2}{b^2}\right)} e^{\left(\frac{-3z^2}{c_f^2}\right)} \quad \text{Eq. 2}$$

$$Q = \mu I V \quad \text{Eq. 3}$$

The Abaqus Welding Interface provides three ways of applying the torch energy to the weld bead.

1. Goldak: Apply body flux to surrounding base material and activated elements based on the Goldak double ellipsoid torch shape. Bead elements are activated at ambient temperature.
2. Constant Temperature: No body flux to surrounding base material or bead elements after activation, but upon activation a body flux is applied to bead elements in order to raise their temperature from ambient temperature to the material's melt temperature.
3. Hybrid: Apply body flux to surrounding base material and activate bead elements at melt temperature, but applied flux during activation to raise temperature to melt temperature.

For this model the Hybrid approach is used. The energy required to melt the entire bead is subtracted from the energy applied via the double ellipsoid body flux in order that the total applied energy matches the input energy.

The element activation is performed through the user subroutine UEPActivationVol(). In order to determine when an element is to be activated, the centroid of the element is projected onto the torch path. When the point of the projection comes within a distance from the center of the torch, equal to an offset scaling parameter times the  $c_f$  parameter, the element is activated. The offset parameter used was 2.0. By activating elements ahead of the torch, the thermal gradients at the front of the torch are reduced and a faster convergence rate in the heat transfer analysis is achieved. This offset parameter is not used when activating elements during the stress analysis.

In this analysis, the initial temperature was 21 C. A convection boundary condition generated a boundary flux on all external surfaces. The total temperature-dependent convection coefficients are computed from Eq. 4 where T is temperature in C.

$$h_c = .0005 + 0.00005 (T - 20) + 6 \times 10^{-10} (T - 20)^3 \quad \text{Eq.4}$$

#### 4. Weld Sequence Controls

The welds are laid down in two separate steps. The first step lays down all of the tack welds simultaneously over a 10 second time period. The second step lays down the remaining beads over a time period of 3160 seconds. The beads are grouped together based on the bead direction with respect to the global Cartesian coordinate system. All of the beads oriented in the x-direction are laid down sequentially. At the same time, all of the beads oriented along the y and z directions are also laid down sequentially. This is equivalent to having three robots simultaneously welding the beads in the x, y, z directions.

The weld sequence is controlled by the user through a dialog box shown in Figure 3. This dialog allows for the customization of each weld pass to define the weld step start time, time to lay the weld, delay time between the passes, and the direction of the pass. The welding time is automatically calculated from the pass length and the torch speed. An option is also available which allows any number of welds to be selected and chosen to be laid down sequentially based on the order in which they were displayed in the table, in this case alphabetically based on the weld name. This helps users to define any variation of weld sequence at minimal preparation effort and therefore faster setup.

This dialog was employed hereby for solving a real weld sequence problem and can be used with different optimization algorithms and Design of Experiment (DOE) matrices to explore the welding design space. Ongoing work of authors integrates this dialog with common evolutionary algorithms such as genetic algorithm in order to find the weld sequence for minimal distortion and as a basis for machine learning practice on control of distortion.

Welding Step Summary - Torch Controls

Step Name: Step\_BeadWelds

Summary Type:  By Weld  By Bead  Highlight selected welds/beads in viewport

Modify	Part Instance Name	Weld Name	Weld Start Time	Time to Lay Entire Weld	Torch Heat Up Time	Interpass Cool Time	Torch Type	Direction	Weld Completion Time
✓	Panel	Left_Bottom_X1_1	945.0	106.0	2.0	2.0	Hybrid	↔	1051.0
✓	Panel	Left_Bottom_X1_2	315.0	106.0	2.0	2.0	Hybrid	↔	421.0
✓	Panel	Left_Bottom_X2_1	421.0	103.0	2.0	2.0	Hybrid	↔	524.0
✓	Panel	Left_Bottom_X3_1	524.0	106.0	2.0	2.0	Hybrid	↔	630.0
✓	Panel	Left_Bottom_Y1_1	505.0	49.0	2.0	2.0	Hybrid	↕	554.0
✓	Panel	Left_Bottom_Y2_1	554.0	47.0	2.0	2.0	Hybrid	↕	601.0
✓	Panel	Left_Bottom_Y3_1	601.0	49.0	2.0	2.0	Hybrid	↕	650.0
✓	Panel	Left_Bottom_Z1_1	246.0	41.0	2.0	2.0	Hybrid	↕	287.0
✓	Panel	Left_Bottom_Z2_1	287.0	41.0	2.0	2.0	Hybrid	↕	328.0
✓	Panel	Left_Lower_X1_1	1051.0	103.0	2.0	2.0	Hybrid	↔	1154.0
✓	Panel	Left_Lower_X1_2	1154.0	106.0	2.0	2.0	Hybrid	↔	1260.0
✓	Panel	Left_Lower_X2_1	1535.0	93.0	2.0	2.0	Hybrid	↔	1628.0
✓	Panel	Left_Lower_X2_2	1628.0	89.0	2.0	2.0	Hybrid	↔	1717.0
✓	Panel	Left_Lower_X2_3	1717.0	93.0	2.0	2.0	Hybrid	↔	1810.0
✓	Panel	Left_Lower_Y1_1	145.0	41.0	2.0	2.0	Hybrid	↕	186.0
✓	Panel	Left_Lower_Y2_1	186.0	38.0	2.0	2.0	Hybrid	↕	224.0
✓	Panel	Left_Lower_Y3_1	224.0	41.0	2.0	2.0	Hybrid	↕	265.0
✓	Panel	Left_Lower_Z1_1	82.0	41.0	2.0	2.0	Hybrid	↕	123.0
✓	Panel	Left_Lower_Z1_2	123.0	41.0	2.0	2.0	Hybrid	↕	164.0
✓	Panel	Left_Lower_Z2_1	559.0	38.5	2.0	2.0	Hybrid	↕	597.5

Total weld step time: 3160.0

Note: All times are step times.

OK Apply Cancel

Figure 3 Weld Summary Dialog.

The parameters used to define the shape of the torch are entered through the Pass Controls dialog (Figure 4). The Pass Controls dialog defines the default time incrementation, torch geometry, and torch energy input parameters. As weld passes are defined, the torch controls are inherited from these default pass controls. For this model. A single set of default parameters is used for all welds.

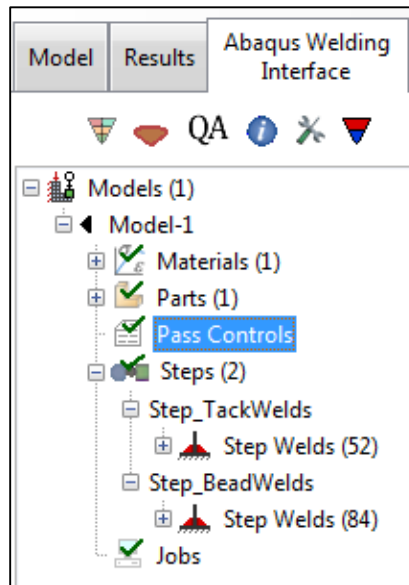


Figure 4 Weld Pass Control for Torch.

An energy measure, the ratio of input-to-melt energy, is provided in the Step Weld dialog (Figure 5). The energy ratio for each weld in this model is approximately 2.8. With typical convection, radiation, and conductive properties this number is often over 5.0. As a result of using the hybrid method of torch application, the underlying base elements will receive less direct energy input than in many welding scenarios than if the pure Goldak heat flux approach were used. This will result in higher temperature gradients during bead element activation as a large percentage of the energy input is required to bring the newly activated elements up to melt temperature.

Pass Number	Bead Name	Torch Speed (mm/sec)	Voltage (Volts)	Current (Amperes)	Efficiency	Input-to-Melt Energy Ratio	Goldak a (mm)	Goldak b (mm)	Goldak cf (mm)	Goldak cr (mm)	Goldak offset
1	Bead-1	5.0	36	400	0.75	2.7763	15	15	15	30	2

Torch Speed (mm/sec)	Voltage (Volts)	Current (Amperes)	Efficiency	Input-to-Melt Energy Ratio
5.0	36	400	0.75	2.7763

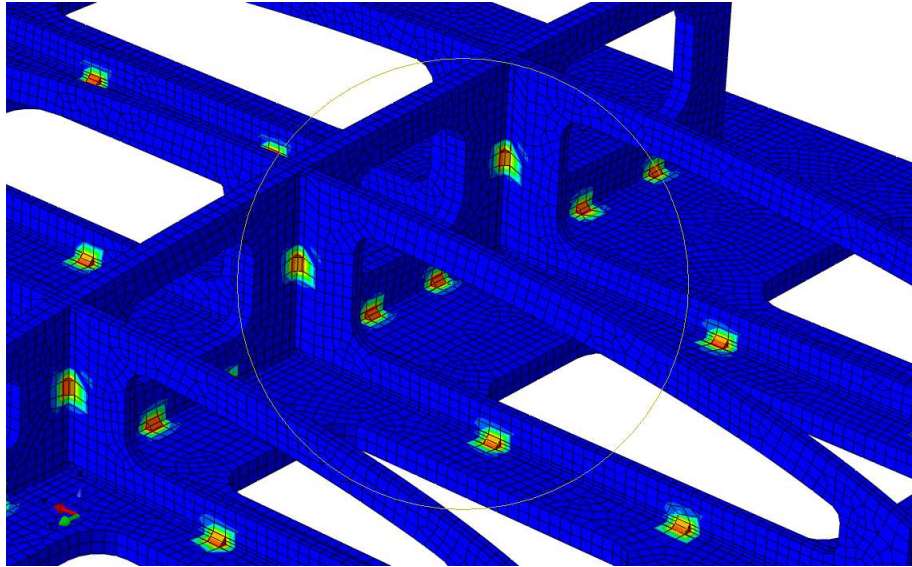
Goldak a (mm)	Goldak b (mm)	Goldak cf (mm)	Goldak cr (mm)	Goldak offset
15	15	15	30	2

Figure 5 Step Weld Dialog.

## 5. Results and Discussion

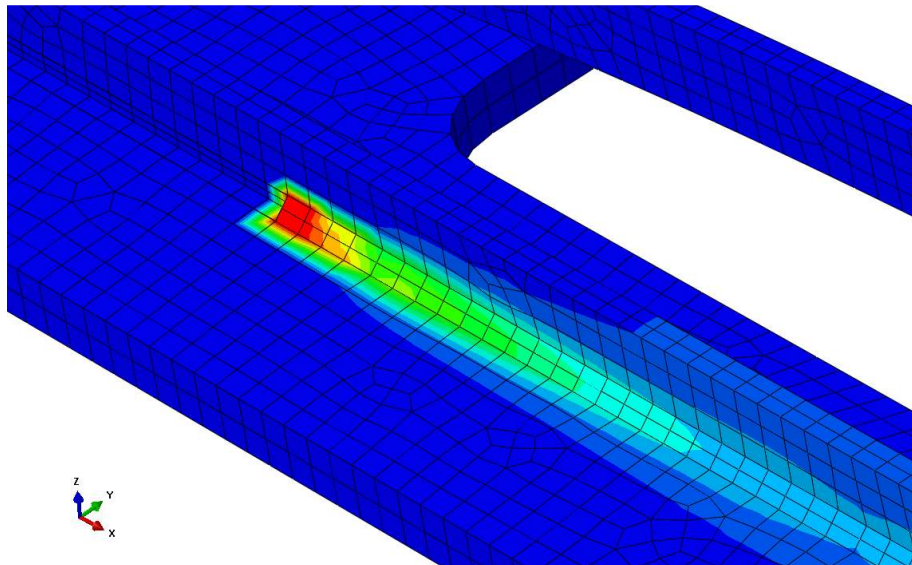
The first step, applying the tack welds (see Figure 6), required 14 increments to complete. The beads were allowed to cool for 2 seconds before the primary weld beads began to be laid down. The temperatures decreased from the activation temperature of 1600°C to around a 1300°C peak by the time the primary welds began to be laid down. There are opinions that recommend to model the tack welds as part of the structure and the welding effect can be ignored. The authors think this is a reasonable trade off of little accuracy for good saving in CPU time. The tack welds, however, are modeled in this project to show the capability of taking the path with better accuracy if required.





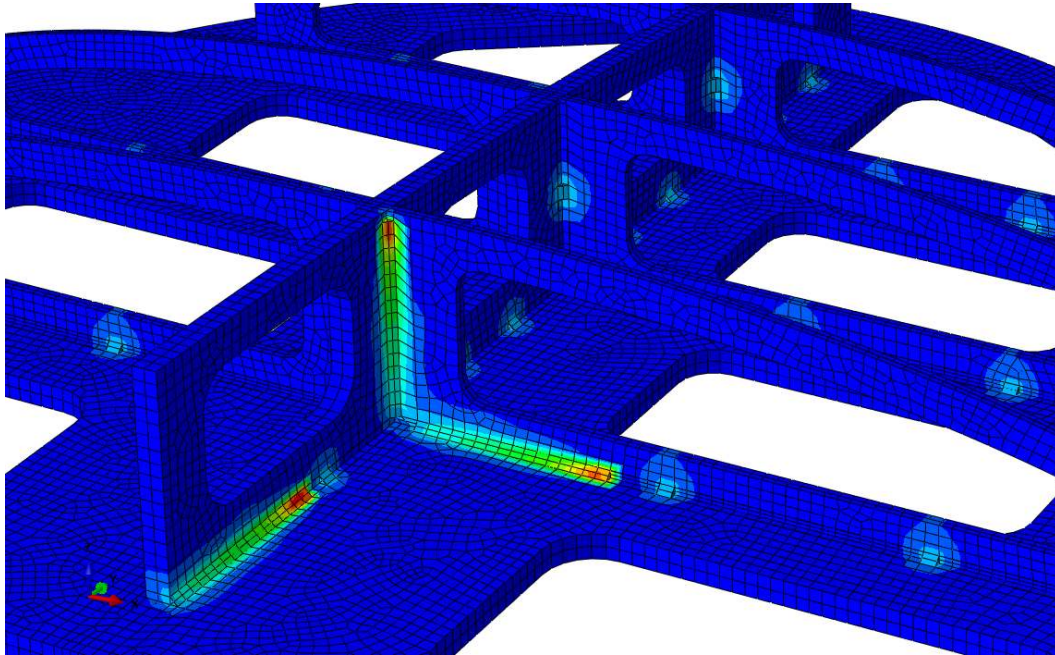
**Figure 6 Tack Weld Temperatures.**

Figure 7 shows the temperature profile just as a group of elements is being activated. The element groups consist of the bead cross-section and one element along the length. Because of the lower input-to-melt energy ratio, the gradients between the activated elements and base elements at element activation are very steep: on the order of  $1400^{\circ}\text{C}$ . With a higher input-to-melt energy ratio, more energy would be put into the base material, thus reducing the large temperature gradients between bead temperature at activation and adjacent element temperatures.



**Figure 7 Temperatures of Bead at Activation.**

Figure 8 shows three of the beads which are being laid down simultaneously. The beads are shown being laid down in a consistent direction. To improve cooling characteristics, the order of the beads could be maintained, but direction of the beads reversed. This would allow region around the start of a bead to cool longer before the placement of the next adjacent bead is begun.



**Figure 8 Three Beads being Laid Simultaneously.**

## 6. Conclusion

The science of welding and the ability to carry out weld analysis are sufficiently advanced to find solutions to complex welding problems e.g. delivering welding with zero distortion. However, the practice of welding engineering remains mostly traditional and based on the science of the pre-computer age. Welding modeling and simulation packages and skills can reduce the gap between the current state of welding science and the actual practice of weld engineering. The Abaqus suite is frequently used in a variety of engineering applications and is therefore suited to provide a common ground for many users to develop the skill of weld modeling. The Abaqus Welding Interface has been shown to have been improved dramatically in the preprocessing area. This is a work in progress, the new energy-based torch flux input and associated user interface dialogs are intuitive and provide a new procedure for matching real world welding input. The weld sequence design is now smoother to prepare and control. However, the continuous element activation may require long run times due to the severe temperature profiles. The next version of AWI will need to include a “chunking” approach to be more efficient.

The authors from Applus Canada received no financial compensation from Simulia (Dassault systemes) for their work helping to develop the AWI. They have no interest in the software beyond the desire to develop the AWI features in order for it to be useful for industrial clients when solving real welding problems.

## 7. References

- Asadi, M., & Goldak, J. (2011). Combinatorial Optimization of Weld Sequence by Using a Surrogate Model to Mitigate a Weld Distortion. *Mechanics and Material in Design*, 123-139.
- Asadi, M., & Goldak, J. (2011). Mitigation of Distortion in an Edge-Welded-Bar by Clamping Parameters. *Int'l Pressure Vessel and Piping Division Conference*. Baltimore, Maryland: ASME.
- Asadi, M., & Goldak, J. (2013). Exploring the Parametric Design Space to Manage Weld Distortion Using Design of Experiment. *Int'l J. of Product Development - Special issue on Simulation-Driven Product Development*, 31-47.
- Asadi, M., Goldak, J., & Weck, A. (2014). Welding Distortion can be Mitigated If Welding Current and Traveling speed Vary Optimized along a Weld Path. *Int'l Pressure Vessels & Piping Division Conference*. Anaheim, CA: ASME.
- Conrardy, C., Huang, T., Harwig, D., Dong, P., Kvidahl, L., Evans, N., & Treaster, A. (2006). Practical Welding Techniques to Minimize Distortion in Lightweight Ship Structures. *Journal of Ship Production*, 239-247.
- Kadivar, M., Jafarpur, M., & Baradaran, H. (2000). Optimizing welding sequence with genetic algorithm. *Computational Mechanics*, 514-519.
- Mochizuki, M., & Toyoda, M. (2006). Weld Distortion Control During Welding Process With Reverse-Side Heating. *Journal of Engineering Materials and Technology*, 265-270.
- Schenk, T., Richardson, I. M., Kraska, M., & Ohnimus, S. (2009). A study on the influence of clamping on welding distortion. *Computational Materials Science*, 999-1005.
- Tsai, C., Park, S., & Cheng, W. (1999). Welding Distortion of a Thin-Plate Panel Structure. *Welding Journal*, 157-195.
- Voutchkov, I., Keane, A., Bhaskar, A., & Olsen, T. (2005). Weld sequence optimization: the use of surrogate models for solving sequential combinatorial problems. *Comput. Methods Appl. Mech. Eng.*, 30-43.
- Wang, H., & Rong, Y. (2008). Case based reasoning method for computer aided welding fixture design. *Computer-Aided Design*, 1121-1132.
- xu, J., & Li, W. (2006). The Nonlinear Time-Varying Response of Dynamic Thermal Tensioning for Welding-Induced Distortion Control. *Journal of Manufacturing Science and Engineering*, 333-341.
- Yang, Y., & Jung, G. (2007). Advancement in Prediction and Control of Welding Residual Stress and Distortion. *Materials Science Forum*, 3943--3948.